RSC Advances

PAPER

View Article Online
View Journal | View Issue

Cite this: *RSC Adv.*, 2026, **16**, 17074

Cooperative flame retardancy of ammonium polyphosphate and magnesium–aluminum-layered double hydroxide (LDH) in EVA blends

Meimei Yu,†[ab] Shuo Qian,†[ab] Yuxin Zuo,*[ab] Yunya Wu,[c] Zhi Li,[d] Zhuo Wang,[e] Zhiqi Liu*[ab] and Pengfei Cheng[f]

To address the issue of excessive magnesium aluminum layered double hydroxides (MgAl-LDH) required in ethylene vinyl acetate copolymer (EVA) to achieve effective flame retardancy, which severely impairs the material's mechanical properties, this study explored the synergistic flame retardant effect of ammonium polyphosphate (APP) and MgAl-LDH. A series of EVA blends were prepared *via* melt blending, with MgAl-LDH as the primary additive and a small amount of APP as the auxiliary flame retardant. The flame-retardant properties, mechanical performance, and char residue characteristics of these blends were systematically evaluated using the limiting oxygen index (LOI) test, UL-94 vertical burning test, cone calorimeter test (CCT), tensile test, and char residue analysis. The results indicated that when the APP content was 8% and the MgAl-LDH content was 47%, the EVA blend achieved a UL-94 V-0 rating, exhibited an LOI value of 29.3%, and demonstrated an elongation at break 52.8% higher than that of the neat EVA (EVA0). This superior performance is primarily attributed to the strong cooperative flame retardant effect of the APP/MgAl-LDH combination, which effectively reduces heat and smoke release during combustion. Furthermore, the incorporation of APP promotes the formation of a dense and continuous char layer on the composite surface, thereby significantly enhancing flame retardant performance. This study is expected to provide a valuable reference for the practical application and green development of flame-retardant EVA materials in the wire and cable industry and construction sector.

Received 2nd February 2026
Accepted 16th March 2026

DOI: 10.1039/d6ra00909c

rsc.li/rsc-advances

1. Introduction

Ethylene-vinyl acetate (EVA) copolymer is a vital thermoplastic elastomer integrating thermoplastic processability and rubber elasticity. It exhibits excellent mechanical properties, weather resistance, electrical insulation, and plasticity, enabling widespread applications. These applications include footwear materials, foamed plastics, wire/cable insulation, photovoltaic encapsulant films, and hot-melt adhesives.[1–4] However, EVA suffers from inherent limitations: poor thermal resistance, low flame retardancy, and significant smoke emission during combustion. Such drawbacks restrict its use in scenarios requiring high fire safety standards.[5,6] Additionally, long-term service may induce thermal-oxidative aging, leading to surface chalking and cracking.

The development of halogen-free flame retardant systems with high efficiency, low smoke, low toxicity, and compatibility with material comprehensive properties is thus critical. This has become a key research focus in materials science.[7,8] To address traditional flame retardant bottlenecks, researchers have explored multifunctional and cooperative systems. Liang *et al.*[9] developed a chitosan (CS)/phytic acid (PA)/polysilsesquioxane (POSS) wood coating *via* layer-by-layer self-assembly. It achieved flame retardancy, antibacterial activity, and hydrophobicity through the Si–O–Si barrier and P–N–Si synergy, with a limiting oxygen index (LOI) of 30.9%. Cheng *et al.*[10] prepared ionic liquid-loaded CuO–ZnO hollow microspheres (CZHS@ILs), which synergized with ammonium polyphosphate (APP) to improve epoxy resin (EP) flame retardancy (LOI = 28, UL-94 V-0: peak heat release rate (pHRR) reduced by 74.8%). C. Baoyu *et al.*[11] developed a composite flame retardant composed of ammonium polyphosphate (APP), carbonized foaming agent (CFA), and layered double hydroxides (LDH) containing rare earth elements (La, Ce, Nd) and applied it to EVA matrix. The system improved the flame retardant performance, reaching the V-0 flame retardant grade and significantly

[a]*College of Chemistry and Chemical Engineering, Anhui University, Hefei 230601, P. R. China. E-mail: zuoyuxin@ahu.edu.cn; lkeyi@126.com*

[b]*Institute of Future Industry Innovation Research, Anhui University, Hefei 230000, P. R. China*

[c]*School of Materials Science and Engineering, Anhui University, Hefei 230601, P. R. China*

[d]*China-Spain Collaborative Research Center for Advanced Materials (CSCRC), School of Materials Science and Engineering, Chongqing Jiaotong University, Chongqing 400074, P. R. China*

[e]*School of Chemical and Process Engineering, University of Leeds, Leeds LS2 9JT, UK*

[f]*Hefei AnYu He New Materials Technology Co., Ltd, Hefei 230088, P. R. China*

† These authors contributed equally to this work.

reducing the heat and smoke release, and maintained the good mechanical properties of the matrix. Chen *et al.*[12] studied the hydrothermal synthesis of magnesium hydroxide (MH) with hexagonal flake morphology and excellent dispersion. After filling it into EVA matrix, the composite achieved excellent flame retardancy (LOI = 49.2%, UL94 V-0) and significantly improved tensile strength at the same time, with a high filling content of 60wt%. Liu *et al.*[13] compared MgAl LDH prepared with different alkali sources and used it with APP for flame-retardant epoxy resin and obtained LDH with larger layer spacing and higher thermal weight loss. The synergistic effect of MgAl-LDH and APP on the heat release and smoke inhibition of EP was the best.

Traditional halogen-based flame retardants release toxic gases and fumes during combustion, endangering human health and damaging equipment.[14–16] Layered double hydroxide (LDH) is a widely used green flame retardant for polymers due to its non-toxic composition.[17–19] Kuila *et al.*[20] prepared sodium dodecyl sulfate (SDS)-intercalated LDH (DS-LDH) and synthesized DS-LDH/EVA nanoblends, which showed improved mechanical properties and thermal stability compared to pure EVA. Du *et al.*[21] inserted pentaerythritol diphosphate (PEDP) into LDH and coated it with melamine resin (MF) to obtain D-LDH@MF, a phosphorus–nitrogen clay flame retardant that enhanced EVA thermal stability.

A major drawback of LDH is its high required addition (>60%) for effective flame retardancy in polymers. This high loading impairs mechanical performance due to poor compatibility between inorganic LDH and polymer matrices.[22] Surface modification of LDH *via* physical adsorption or chemical reaction is a common solution to improve dispersion. Y. Feng *et al.*[23] modified magnesium hydroxide (MH) with silanes (KH550, KH570), stearic acid, or titanate and incorporated it into EVA/PE blends, achieving better dispersion and flame retardancy. However, organic modifiers are often flammable, limiting mechanical property improvements and potentially reducing flame retardancy.[24]

APP is a key halogen-free flame retardant; its thermal decomposition produces ammonia and polymeric phosphoric acid, which shield polymers from oxygen.[25,26] Ji[27] uniformly dispersed MgAl-LDH and APP in butadiene vinyl rubber/EVA (SBR/EVA) foam cavity walls using epoxy resin and foaming agents. This constructed an insulating layer that reduced initial heat release rate and flammable gas emission. Wang *et al.*[28] prepared microencapsulated APP with melamine–formaldehyde or epoxy resin shells, which significantly enhanced EVA flame retardancy when added alone or with pristine APP.

Recent studies have focused on the flame retardant performance of the APP/LDH combination. It has been confirmed that APP can improve material mechanical properties while reducing heat and smoke emissions.[29–31] EVA blends were prepared *via* melt blending. EVA acted as the polymer matrix, with magnesium–aluminum layered double hydroxide (MgAl-LDH) as the primary flame retardant and ammonium polyphosphate (APP) as the co-flame retardant. The flame retardant and smoke suppression properties of the blends were evaluated using the limiting oxygen index (LOI) test, the cone calorimeter test (CCT), and the vertical burning test. These characterizations aimed to investigate the cooperative flame retardant effect of the MgAl-LDH/APP combination. The optimal mass ratio of MgAl-LDH to APP was determined to maximize flame retardancy through their cooperative interaction. This study provides a feasible strategy for the rational utilization of MgAl-LDH. It also offers a more economical and efficient approach for developing halogen-free flame retardant EVA materials with promising application potential. Additionally, the findings shed new light on the efficient flame retardant modification of LDH-based polymer composites.

2. Experimental part

2.1. Materials

Ethylene-vinyl acetate (EVA, grade 265, VA content 28 wt%) copolymer was supplied by DuPont (USA). Magnesium–aluminum layered double hydroxide (MgAl-LDH, Mg/Al molar ratio 2.6, specific surface area 8–12 $m^2\ g^{-1}$) was provided by Hefei AnYuHe New Materials Technology Co., Ltd (China), The employed MgAl-LDH exhibits a sub-micron particle size distribution and high specific surface area (Fig. S4), which contributes to its surface activity and dispersion within the polymer matrix. Ammonium polyphosphate (APP, crystalline form II, P_2O_5 > 68 wt%) was purchased from Shandong Yusuo Chemical Technology Co., Ltd (China). MC226 (a maleic anhydride grafted polyethylene (PE-g-MA) compatibilizer, was used to improve the interfacial adhesion between the hydrophilic flame retardants and the hydrophobic EVA matrix) was obtained from Ningbo Nengzhiguang New Material Technology Co., Ltd (China).

2.2. Instruments and equipment

The instruments and equipment employed in this work included a mixing torque rheometer (Harbin Harper Electric Technology Co., Ltd, China), a thermogravimetric analyzer (TGA, TA Instruments, USA), a flat-plate vulcanizing machine (Xihua Instrument Testing Co., Ltd, China), a pneumatic slicer (Xihua Instrument Testing Co., Ltd, China), a cone calorimeter (CCT, Mortise Combustion Technologies Ltd, UK), an X-ray diffractometer (XRD, Hitachi Rigaku Corporation, Japan), and a cold field emission scanning electron microscope (SEM, Hitachi Manufacturing Co., Ltd).

2.3. Preparation of EVA blends

EVA and its composite blends were fabricated *via* a melt blending approach. Prior to processing, EVA was dried at 60 °C for 2 h, whereas APP and LDH were dried at 110 °C for 5 h to eliminate moisture interference. Initially, EVA and the compatibilizer MC226 were charged into a torque rheometer, followed by mixing at 150 °C with a rotational speed of 35 rpm. The chemical compositions of LDH, APP, and the resultant composites were verified *via* FTIR, with corresponding spectra provided in Fig. S1. After the complete melting of EVA, the APP/LDH flame-retardant systems with varying mass ratios were incorporated according to the formulations listed in Table 1.

Table 1 Compositions, limiting oxygen index (LOI), and UL-94 ratings of pure EVA and its blends with varying APP/LDH ratios at a fixed total flame retardant loading of 55 wt%

Samples	EVA/wt%	LDH/wt%	APP/wt%	MC226/wt%	LOI/%	UL94
Pure EVA	95	0	0	5	22.3	HB
EVA0	40	55	0	5	34.6	V-0
EVA1	40	53	2	5	32.6	V-0
EVA2	40	51	4	5	30.6	V-0
EVA3	40	49	6	5	30.2	V-0
EVA4	40	47	8	5	29.3	V-0
EVA5	40	45	10	5	28.7	V-1
Pure APP	40	0	55	5	25.8	V-0

The mixtures were further blended for 10 min to yield homogeneous composite materials. Subsequently, the as-prepared composites were cut into small pieces, placed in a plate vulcanizer, and hot-pressed into uniform sheets. Finally, the sheets were trimmed into standard test specimens using a pneumatic slicer for subsequent characterization.

The HB level in UL94 standard is the lowest flame retardant level in the flammability test of plastic materials, that is, there is basically no flame retardant capacity.

2.4. Characterization methods

The mechanical properties test was conducted on a universal testing machine (Shenzhen Sansi Zongheng Technology Co., Ltd). The test option was designed to determine the tensile properties of molded and extruded plastics. The speed of the testing machine is was mm min^{-1}, the extensometer gauge length was 25 mm, and the dumbbell-shaped sample dimensions was 115 × 6 × 1.6 mm (dumbbell-shaped). The thermogravimetric test was performed using a TG55 from TA, USA. The test was conducted under an experimental atmosphere of N_2, with a heating rate of 20 °C min^{-1} and a heating span of 40–800 °C. The LOI is tested in accordance with the GB/T 2406.1-2008 on an oxygen index combustion tester from Modis Technology Co., Ltd. The flame retardant rating has been determined using a UL94 horizontal and vertical combustion tester from Mortis Technologies Ltd. The spline dimension was 125 × 13 × 3 mm. A cone calorimeter was used to evaluate the smoke suppression performance of the samples. The test was conducted at a heat flux density of 50 kW m^{-2}, and the samples had dimensions of 100.0 × 100.0 × 3.0 mm. To prove the compatibility between resin and additives, the SEM of the LDH, APP, and compound are presented in Fig. S2.

3. Results and discussion

3.1. Mechanical properties test of EVA blends

Fig. 1 presents the tensile strength and elongation at break of neat EVA and EVA blends with varying APP loadings. The variance of the tensile test results for all formulations is reported in Table S1. The results indicate that the elongation at break of the blends increases with increasing APP content, increasing from 82.5% for EVA0 to 134.1% for EVA5. Conversely, the tensile strength of the EVA blends decreases with increasing APP loading, declining from 11.68 MPa for EVA0 to 9.69 MPa for EVA5. APP functions as a toughening agent in the EVA matrix, thus accounting for the elevated elongation at break with increasing APP content. Nevertheless, high elongation at break—an indicator of the material's ability to withstand large deformations—induces localized necking during tensile testing. This necking effect triggers stress concentration within the matrix, ultimately leading to material fracture. Accordingly, a more pronounced necking phenomenon corresponds to the lower tensile strength of the EVA blends.[32]

3.2. Thermal stability of EVA blends

Thermogravimetric analysis (TGA) was employed to investigate the thermal degradation behavior of EVA-based materials. The thermal degradation data of neat EVA and EVA/LDH/APP composites with varying APP loadings are summarized in Table 2 and Fig. 2. Thermal stability is a critical property for flame-retardant polymer materials as it is primarily governed by the release of decomposition products and char formation efficiency during thermal exposure.

As illustrated in Fig. 2(a), neat EVA initiates thermal degradation at 322.77 °C and undergoes a two-stage decomposition process. The first decomposition stage occurs at 367.18 °C, which is attributed to the cleavage of carboxylic acid groups, while the second stage takes place at 489.14 °C, corresponding to the breakdown of ethylene backbone chains. Notably, the char residue of neat EVA at elevated temperatures (up to 800 °C) is nearly negligible. In order to understand the role of LDH in composites, the thermal behavior of LDH was analyzed. As shown in Fig. 2, the TGA-DTG curve of MgAl-LDH shows typical multi-stage decomposition characteristics. The initial weight loss temperature (T1%) is 230.91 °C, which corresponds to the removal of physical adsorption water and part of interlayer water. In the first stage, the maximum weight loss peak (T_{max1}) appeared at 297.63 °C, mainly due to the hydroxyl removal of the laminate. The second stage maximum weight loss peak (T_{max2}) is located at about 399.21 °C, which is related to the decomposition of interlayer carbonate ions and further structural dehydration. In some tests, the third stage of weight loss (T_{max3}) can be observed at 491.2 °C, representing the complete conversion to mixed metal oxides (MgO, Al_2O_3). After high temperature of 800 °C, the char yield of pure LDH reached

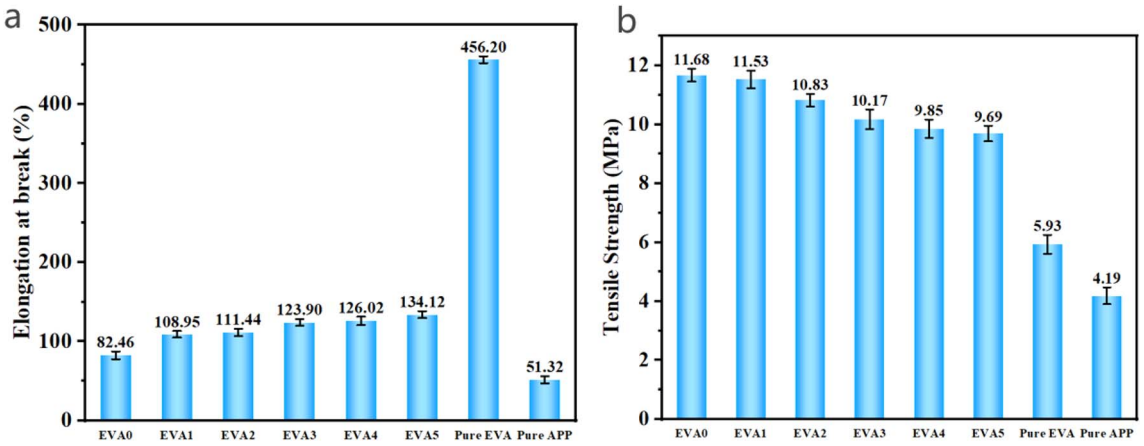

Fig. 1 Effect of varying APP/LDH ratios on the mechanical properties of EVA blends: (a) elongation at break; (b) tensile strength.

Table 2 Characteristic thermal decomposition data and residual char yields from TGA for EVA

Samples	$T1\%$/°C	T_{max1}/°C	T_{max2}/°C	T_{max3}/°C	Char yield/%
Pure EVA	322.77	—	367.18	489.14	0.11
EVA0	230.91	297.63	399.21	491.20	30.89
EVA1	231.24	294.59	394.67	493.22	31.36
EVA2	225.72	294.09	392.53	496.81	31.61
EVA3	217.46	286.73	386.57	497.11	31.79
EVA4	234.41	297.93	398.41	500.51	31.93
EVA5	222.19	293.73	383.03	499.53	32.92
Pure APP	338.83	—	353.64	469.49	30.41

30.89%, which was mainly due to the thermal stable metal oxides formed by its decomposition.

With the incorporation of LDH into the EVA matrix, the initial decomposition temperature (IDT) of the composite decreases to 230.91 °C, which is substantially lower than that of neat EVA. This phenomenon arises from the abundant interlayer water and hydroxyl (–OH) groups in the LDH structure, which release structural water (H_2O) and carbon dioxide (CO_2) at relatively low temperatures, thereby triggering the premature thermal decomposition of the EVA matrix. Despite lowering the IDT, the release of these non-combustible gases dilutes the concentration of flammable volatiles, thus exerting a gas-phase flame-retardant effect. The char residue of the EVA0 composite at 800 °C increases to 30.89%, endowing the material with inherent flame-retardant properties. Furthermore, the char residue rates of EVA ternary blends containing both APP and LDH are higher than those of EVA0. This enhancement stems from the thermal decomposition of APP to form polyphosphoric acid, which catalyzes the dehydration and cross-linking of the EVA matrix to generate an intumescent char layer. Concurrently, LDH decomposes to produce metal oxides (MgO, Al_2O_3), which react with polyphosphoric acid to form thermally stable metal phosphates. These phosphates reinforce the mechanical strength and thermal stability of the char layer. Synergistically, APP and LDH cooperate to construct a dense, continuous composite protective barrier, which effectively isolates heat and oxygen penetration while suppressing the release of flammable volatiles. This synergistic effect elevates the char residue rate, highlighting the prominent condensed-phase flame-retardant

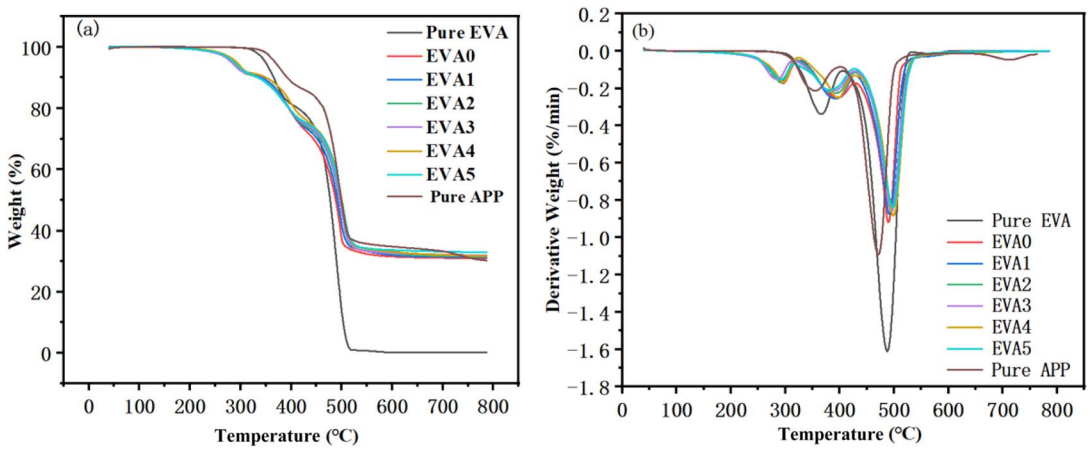

Fig. 2 Thermal degradation behavior under N_2 atmosphere: (a) TGA and (b) DTG curves of EVA blends with varying APP/LDH ratios.

efficiency of the hybrid system. This finding further corroborates the existence of a distinct synergistic flame-retardant interaction between APP and LDH.[33]

As shown in Fig. 2(a), the EVA composite undergoes a three-stage weight loss process during TGA testing. The initial weight loss stage is associated with the evaporation of weakly bound interlayer water from the LDH component within the composite. The subsequent two decomposition stages involve dehydroxylation and decarbonylation reactions in the LDH crystal lattice, along with the cleavage of acetic acid groups in the EVA side chains and the fragmentation of the EVA main chain. Moreover, EVA0 exhibits a faster decomposition rate than neat EVA in the first two stages, whereas its decomposition rate slows down in the third stage. This trend is ascribed to the accelerated cleavage of carboxylic acid groups induced by LDH, which, in turn, reduces the decomposition rate during the final stage of thermal degradation.[34]

The derivative thermogravimetry (DTG) curves presented in Fig. 2(b) provide further insight into the degradation kinetics and the synergistic effect between APP and LDH. For the LDH-filled composite (EVA0), three distinct peaks corresponding to the aforementioned stages are observed at 297.63, 399.21, and 491.20 °C, respectively. The first peak is attributed to the loss of interlayer water from LDH, while the second and third peaks correspond to the deacetylation of EVA and the main-chain scission, overlapping with LDH dehydroxylation.

Remarkably, the addition of APP significantly alters the DTG profile. As shown in Fig. 2(b), with increasing APP content (*e.g.*, from EVA1 to EVA5), the second decomposition peak (T_{max2}, associated with EVA deacetylation) shifts to lower temperatures initially, then stabilizes or slightly increases for optimal formulations (*e.g.*, 398.41 °C for EVA4). More importantly, the third decomposition peak (T_{max3}, representing the most thermally stable component and the integrity of the char layer) shows a consistent and notable shift to higher temperatures. As listed in Table 2, the final-stage decomposition temperature (T_{max3}) of the optimal composite EVA4 (500.51 °C) is not only 9.3 °C higher than that of the LDH-only composite EVA0 (491.20 °C) but also substantially exceeds that of the APP-only sample (469.49 °C). This consistent increase in T_{max3} for the blends, surpassing both individual components, strongly indicates the formation of a more thermally stable char residue due to the interaction between APP-derived phosphoric acids and LDH-derived metal oxides. Similarly, the char residue at 800 °C for EVA4 (31.93%) is higher than that of EVA0 (30.89%), suggesting that APP enhances the char-forming efficiency of the LDH system, rather than simply providing an additive effect. The TGA and derivative thermogravimetry (DTG) curves of LDH, APP, and the resultant composites (EVA4) are provided in Fig. S3.

T1% represents the temperature at 1% mass loss. T_{max1}, T_{max2}, and T_{max3} correspond to the temperatures of the maximum mass loss rate in the first, second, and third decomposition stages, respectively.

3.3. LOI and UL94 of EVA blends

The LOI and UL 94 tests are widely adopted to evaluate the fire resistance of materials and optimize flame-retardant formulations.[35] Table 1 summarizes the LOI values and UL 94 classification data for EVA blends with varying APP loadings. As presented in Fig. 1, the LOI of EVA composites containing 55 wt% LDH increases remarkably from 22.3% to 34.6% relative to neat EVA. Because the ratio of MgAl-LDH decreases, the LOI of the composites decreases; however, the addition of APP forms a significant condensed phase synergy with LDH through strong catalytic charring such that the material can still maintain excellent overall flame retardant performance after the addition of LDH is reduced (UL-94 V-0: significantly reduced heat/smoke release). This variation in fire performance is attributed to the gradual reduction in LDH content in the EVA0–EVA5 series. Upon thermal exposure, LDH undergoes thermal decomposition, releasing H_2O and CO_2. These non-combustible gases dilute the concentration of flammable volatiles, reduce the combustion temperature, and generate metal oxide residues that physically inhibit combustion by blocking oxygen diffusion.[36] Although APP also releases non-combustible gases during thermal degradation, its flame-retardant efficiency is less pronounced than that of LDH.

During combustion, the incorporation of APP into the EVA composite facilitates the cross-linking of the polymer matrix and promotes its carbonization. This subsequently induces the formation of a dense, intact char layer on the material surface. Serving as an efficient thermal barrier, the char layer effectively shields the underlying polymer matrix, thereby reducing the pyrolysis rate and suppressing the generation of flammable volatiles.[37]

3.4. Combustion behavior of EVA blends

Cone calorimetry testing (CCT) is a widely utilized technique for characterizing the combustion behavior of materials, and it is routinely employed to evaluate their smoke and heat suppression performance.[38] Despite its small-scale operation, previous studies have verified that CCT results exhibit strong consistency with those obtained from full-scale fire tests, thus validating its effectiveness for predicting the combustion behavior of materials under real-fire conditions.[39] In the present work, a cone calorimeter was used to assess the fire performance of neat EVA and EVA blends with varying APP/LDH ratio loadings.

Fig. 3 presents the heat release rate (HRR) and total heat release (THR) profiles of neat EVA and EVA blends with different APP/LDH ratios. As shown in Fig. 3(a), neat EVA exhibited a peak HRR (pHRR) of 862.9 kW m^{-2} at 110 s, with complete combustion occurring at 187 s. The unimodal HRR profile of neat EVA is indicative of combustion without char formation. For the EVA composite with LDH added alone, the HRR decreased significantly and exhibited a bimodal distribution. The first peak (250.9 kW m^{-2}) emerged at 115 s, corresponding to the initial combustion of the polymer matrix. In contrast, the second peak (209.7 kW m^{-2}) at 300 s was attributed to the cracking of the fragile char layer under sustained thermal exposure. With the incorporation of APP to adjust the APP/LDH ratios, the HRR curves of EVA blends also displayed bimodal characteristics: the first peak appeared earlier than that of the LDH-only composite, while the second peak was delayed. This

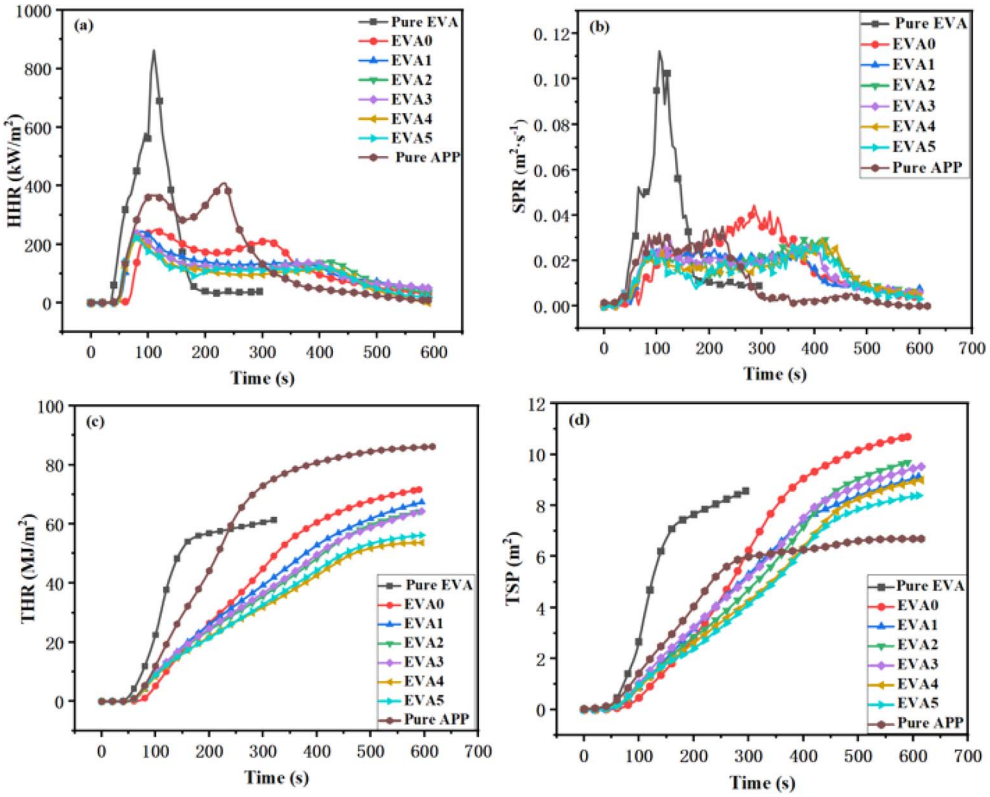

Fig. 3 Cone calorimeter test results of EVA blends with different APP/LDH ratios: (a) heat release rate (HRR), (b) total heat release (THR) at 300 s, (c) smoke production rate (SPR), and (d) total smoke production (TSP) at 300 s.

phenomenon confirms that APP addition catalyzes the formation of a robust, dense char layer, which more effectively blocks the diffusion of flammable volatiles into the combustion zone. As illustrated in Fig. 3(b), the THR of EVA blends at 300 s decreased from 60.56 MJ m^{-2} (neat EVA) to 44.96 MJ m^{-2} (EVA0) and was further reduced to 31.90 MJ m^{-2} with 8 wt% APP loading. The introduction of APP thus further lowered the HRR and effectively diminished the total heat output of EVA blends throughout the combustion process. The reduction in THR values demonstrates a distinct synergistic flame-retardant effect between APP and LDH, which significantly enhances the fire resistance of EVA blends and yields a superior flame-retardant performance.

Fig. 3 also depicts the smoke production rate (SPR) and total smoke production (TSP) curves of neat EVA and EVA blends with different APP/LDH ratios during combustion. As shown in Fig. 3(c), neat EVA exhibited rapid and extensive smoke release after ignition, with a peak SPR of 0.112 m^2 s^{-1} at 105 s. The EVA composite containing only LDH reached a maximum SPR of 0.044 m^2 s^{-1} at 285 s. With the gradual incorporation of APP (the proportion of LDH decreases accordingly), the SPR curves of EVA blends also showed bimodal behavior. The first peak originated from smoke generated during the initial combustion of the polymer matrix, while the second peak was caused by the cracking of the char layer, which was insufficiently robust to withstand prolonged burning, after APP-induced carbonization. The first SPR peak appeared at 90 s, which was associated with the surface combustion of the material; this earlier onset indicates that APP accelerates the charring process of the EVA matrix. Compared with LDH, APP acts as both a charring catalyst and a char-layer reinforcer, resulting in the second SPR peak occurring later and with lower intensity after material combustion. The second SPR peak of the APP-containing blends emerged at approximately 415 s, with a maximum value of 0.0088 m^2 s^{-1}; this was attributed to the enhanced thermal stability of the char layer formed during combustion. As shown in Fig. 3(d), the TSP of EVA composites at 300 s decreased from 8.59 m^2 (neat EVA) to 6.24 m^2 (EVA0) and was further reduced to 4.26 m^2 with 8 wt% APP loading. This result highlights the role of APP in accelerating the early-stage degradation of the polymer matrix and promoting the formation of a continuous, dense char layer, thereby effectively suppressing smoke emission during combustion.[40]

In Table 3, the time to ignition (TTI) of all EVA composites is significantly longer than that of pure EVA. Among them, the TTI of EVA0 is the longest, which is attributed to the delayed effect of endothermic LDH decomposition and gas dilution on ignition. After adding APP, TTI was shortened, which was because while APP promoted the early degradation and charring reaction, it also helped to form a protective carbon layer earlier in the process, thus changing the combustion process. Fire growth rate index (FIGRA: ratio of peak heat release rate pHRR to time to peak) is a key index for assessing fire risk. All samples containing flame retardant FIGRA (2.18–2.97 kW $[m^2$ $s]^{-1}$) were far

Table 3 Key parameters from cone calorimeter tests of EVA blends with different APP/LDH compositions (50 kW m^{-2})[a]

Samples	TTI (s)	pHRR (kW m^{-2})	pSPR (m^2 s^{-1})	THR (MJ m^{-2}) at 300 s	TSP (m^2) at 300 s	FIGRA (kW [m^2 $s]^{-1}$)	Char yield (%)
Pure EVA	31	862.9	0.112	60.56	8.59	7.84	0
EVA0	64	250.9	0.044	44.96	6.24	2.18	11.68
EVA1	47	243.6	0.025	39.36	5.30	2.87	12.98
EVA2	45	232.3	0.029	35.64	4.73	2.73	13.69
EVA3	45	237.6	0.029	36.70	4.20	2.97	13.58
EVA4	47	221.9	0.029	31.90	4.26	2.77	13.57
EVA5	45	222.3	0.027	32.87	4.13	2.78	13.97
Pure APP	43	414.4	0.035	72.95	5.99	1.78	65.84

[a] Char yield is the residual mass percentage at 800 °C.

lower than pure EVA (7.84 kW [m^2 $s]^{-1}$). The FIGRA of EVA4 is 2.77 kW [m^2 $s]^{-1}$, which is at a low level, indicating that its fire risk is significantly reduced and its combustion growth is slow. The residual carbon rate directly reflects the flame retardant effect of the condensed phase. With the partial substitution of APP for LDH, the carbon residue rate of the composite increased from 11.68% for EVA0 to 13.97% for EVA5. This directly confirms the synergy of APP and LDH in promoting carbon formation: APP catalyzes the formation of a carbon layer, while LDH decomposition products enhance the carbon layer, leading to more stable carbon residue.

3.5. Analysis of carbon layer structure of EVA blends

Fig. 4 displays the char residue morphologies of neat EVA and EVA blends with varying APP loadings after cone calorimetry testing (CCT). For the EVA composite containing only LDH, minor surface cracking is observed post-combustion, with no distinct char layer formed. In contrast, the incorporation of APP results in a well-defined char layer on the blend surface, and the coverage area of this char layer expands progressively with increasing APP content. During combustion, APP decomposes to generate phosphoric acid and hypophosphorous acid. These species promote the dehydration and carbonization of combustible components within the EVA matrix. The high-quality condensed-phase char layer effectively isolates the underlying polymer from the external environment, thereby significantly suppressing the further combustion of the internal matrix, reducing the emission of flammable volatiles, and conferring excellent smoke suppression performance to the composites.[41] From the SEM, it can be seen that the compactness of the residual carbon added with APP is higher than that without APP, and the compactness gradually increases with the increase in APP quantity. This is because when APP and LDH coexist, the metal oxides released by LDH at high temperatures can react with the phosphate formed by APP pyrolysis to form metal phosphate. These products can further enhance the high temperature resistance of the carbon layer, make it more compact, and reduce the generation of cracks.

The synergistic flame-retardant mechanism of APP and Mg–Al layered double hydroxide (Mg–Al-LDH) is elucidated as follows. First, condensed-phase synergy serves as the core mechanism, which enhances catalytic char formation: polyphosphoric acid derived from the thermal decomposition of APP catalyzes the dehydration and cross-linking of the polymer matrix to form an intumescent char layer. Meanwhile, metal

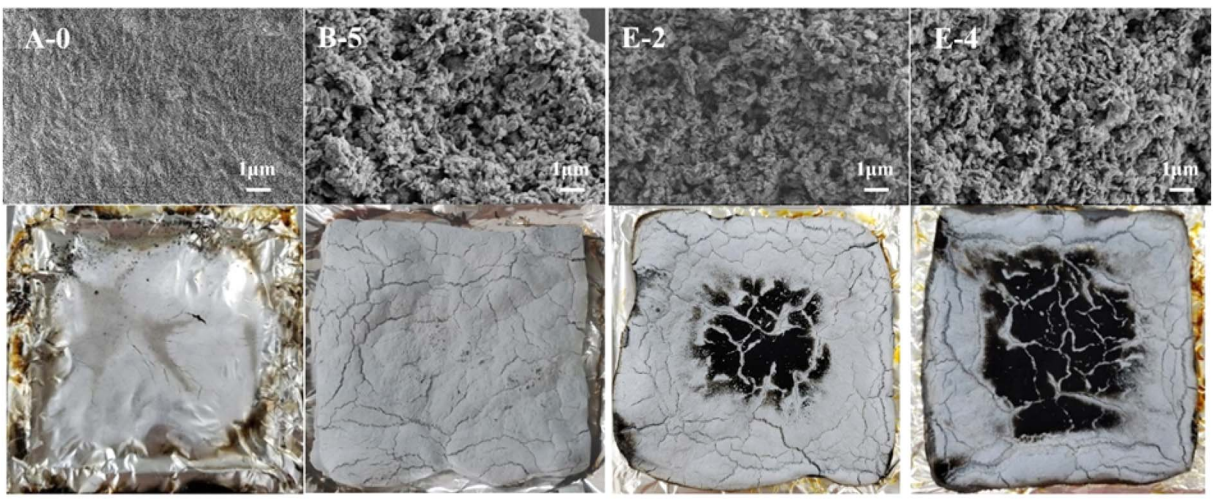

Fig. 4 SEM and digital photographs of the residues after cone calorimetry tests for (A-0) pure EVA, (B-5) EVA0, (E-2) EVA3, and (E-4) EVA5.

oxides (MgO, Al_2O_3) generated by the thermal decomposition of Mg–Al-LDH react with polyphosphoric acid to form thermally stable metal phosphates. These phosphates contribute to the construction of a robust, dense, and continuous composite protective barrier that effectively blocks heat and oxygen transfer to the underlying polymer matrix and inhibits the release of flammable volatiles. Second, gas-phase synergy complements the condensed-phase effect: the decomposition of Mg–Al-LDH releases water vapor (H_2O) and carbon dioxide (CO_2), which dilute the concentrations of oxygen and flammable gases in the combustion zone, thereby interrupting the combustion chain reaction. Concurrently, the thermal decomposition of APP is an endothermic process that absorbs substantial heat. It also releases ammonia (NH_3) and other non-combustible gases, which further enhance the gas-phase dilution effect. Collectively, the endothermic decomposition processes of APP and Mg–Al-LDH absorb significant heat, effectively cooling the polymer matrix and decelerating its pyrolysis rate.[42,43]

3.6. XRD analysis of char residue after CCT

The CCT simulates real-fire conditions by exposing materials to controlled heat flux, leading to combustion and char formation. The char layer plays a critical role in flame retardancy by acting as a physical barrier that insulates the underlying polymer from heat and oxygen. Analyzing the char residue after CCT provides insights into the structural and compositional changes induced during combustion. XRD is particularly useful for characterizing the crystalline phases within the char as it can identify the formation of metal oxides, phosphates, and other compounds that contribute to the stability and effectiveness of the char layer. By performing XRD on the post-combustion residues, we can elucidate the condensed-phase flame-retardant mechanisms and validate the synergistic interactions between APP and Mg–Al-LDH.

Fig. 5 shows the XRD patterns of the char residues from pure EVA and EVA blends with varying APP additions after CCT. The XRD patterns reveal distinct peaks corresponding to crystalline phases formed during combustion. For pure EVA, the absence of significant crystalline peaks indicates that the material burns completely without forming a stable char layer. In contrast, the EVA0 sample (containing 55% LDH) exhibits peaks characteristic of metal oxides, which are decomposition products of LDH. These metal oxides contribute to the formation of a residual char layer, albeit with limited structural integrity, as evidenced by minor cracking observed in the digital photographs (Fig. 4).

With the incorporation of APP, the XRD patterns of the blends (EVA1 to EVA5) show additional peaks corresponding to metal phosphates. These compounds are formed through reactions between polyphosphoric acid (released from APP decomposition) and metal oxides (from LDH decomposition). The presence of metal phosphates enhances the thermal stability and mechanical strength of the char layer, leading to a denser and more continuous protective barrier. This is consistent with the observed improvements in flame retardancy, such as reduced heat release rate (HRR) and smoke production (Fig. 3).

In contrast to pure EVA and EVA0, the incorporation of APP significantly altered the morphology and composition of the char residue. To further elucidate these changes, the XRD pattern of the optimal EVA4 blend (47 wt% LDH, 8 wt% APP) is examined in detail (Fig. 5). It shows distinct crystalline diffraction peaks at approximately $2\theta = 43.0°$, 62.5°, and 78.7°, which can be indexed to the (200), (220), and (222) crystal planes of cubic periclase-structured magnesium oxide (MgO, ICDD PDF card no. 79-0612). This confirms that during combustion, the MgAl-LDH additive underwent thermal decomposition, ultimately forming crystalline MgO as a stable solid residue within the char layer. The presence of such well-defined, crystalline metal oxides significantly contributes to the mechanical strength and thermal stability of the protective char barrier.[44] The formation of crystalline MgO is a key outcome of the cooperative flame-retardant mechanism. The metal oxides (MgO and Al_2O_3) derived from LDH decomposition can react with polyphosphoric acid (generated from APP thermal decomposition) to form thermally stable metal phosphates.[45] While the characteristic peaks of such phosphates or Al-containing phases might overlap or be less intense in the patterns of EVA1 to EVA5, the prominent MgO peaks in EVA4 provide direct evidence of the condensed-phase actions of LDH and its synergistic interaction with APP in reinforcing the char structure.

The intensity of the carbon-related peaks in the XRD patterns increases with higher APP content, indicating enhanced carbonization and cross-linking within the char layer. This aligns with the conclusions drawn from the digital photographs (Fig. 4), where the char layer coverage expands with increasing APP addition. The synergistic interaction between APP and MgAl-LDH promotes the formation of a composite protective layer comprising carbon, metal oxides, and metal phosphates, which effectively isolates the polymer matrix from external heat and oxygen.

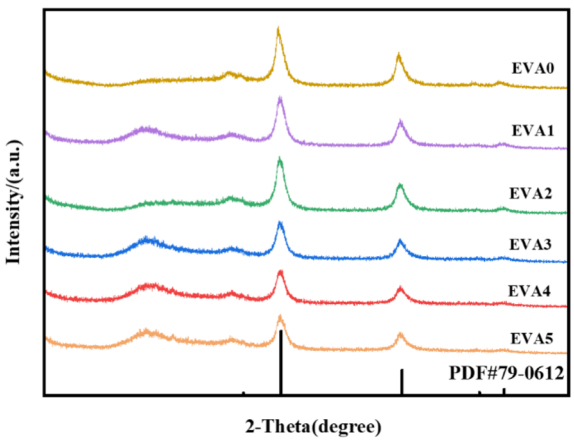

Fig. 5 XRD patterns of the char residues from EVA blends with different APP/LDH ratios after cone calorimetry tests.

4. Conclusion

This study incorporated ammonium polyphosphate and magnesium–aluminum layered double hydroxide into ethylene-vinyl acetate copolymer at a specific mass ratio for flame retardant modification. The effects of the composite flame retardant on the thermal stability, mechanical properties, and flame retardancy of the blends were investigated. When ammonium polyphosphate and magnesium–aluminum layered double hydroxide accounted for 47% and 8%, respectively (EVA4), the flame retardancy of the composite was significantly improved. It achieved a UL94 V-0 rating without dripping and a limiting oxygen index of 29.3%. The cooperative effect between ammonium polyphosphate and magnesium–aluminum layered double hydroxide in ethylene-vinyl acetate copolymer significantly reduced heat release and smoke release after 300 seconds of combustion. Heat release decreased from 60.56 MJ m^{-2} for pure ethylene-vinyl acetate copolymer to 31.90 MJ m^{-2} for EVA4. Total smoke production (TSP) decreased from 8.59 m^2 to 4.26 m^2 at 300 seconds. In addition, ammonium polyphosphate promoted the formation of a dense and intact char layer. This further enhanced flame retardant and smoke suppression performance. Through cooperative catalytic carbonization, the flame retardant efficiency of ammonium polyphosphate in the ethylene-vinyl acetate copolymer magnesium–aluminum layered double hydroxide system was significantly improved. This study confirms that,when APP is mixed with MgAl-LDH in an appropriate proportion, compared with single LDH or single APP, it can significantly reduce the heat release rate (pHRR from 250.9 to 221.9 kW m^{-2}), total heat release and smoke generation of EVA composites while maintaining UL-94 V-0 grade, and improve the thermal stability of residual carbon (T_{max3} increases by about 9 °C). The advantages of these performance indicators show that there is a clear synergistic flame retardant effect between APP and LDH.

Author contributions

Validation, Meimei Yu and Shuo Qian; formal analysis, Meimei Yu and Shuo Qian; resources, Meimei Yu; data curation, Meimei Yu, Shuo Qian, and Zhuo Wang; writing—original draft, Meimei Yu; writing—review and editing, Zhiqi Liu, Shuo Qian, Yunya Wu, Yuxin Zuo, Zhi li, and Pengfei Cheng; supervision, Zhiqi Liu, Yuxin Zuo, Zhi Li, Yunya Wu, and Pengfei Cheng; project administration, Zhiqi Liu and Yuxin Zuo; funding acquisition, Zhiqi Liu. All authors have read and agreed to the published version of the manuscript.

Conflicts of interest

Author Pengfei Cheng was employed by the company Hefei AnYuHe New Materials Technology Co., Ltd. The remaining authors declare that the research was conducted in the absence of any commercial or financial relationships that could be construed as a potential conflict of interest.

Data availability

The original contributions presented in this study are included in the article. Further inquiries can be directed to the corresponding authors.

Supplementary information (SI): Fig. S1: The FTIR of LDH, APP, and compound; Fig. S2: The SEM of (a) LDH, (b) APP, and (c) compound; Fig. S3: (a) TGA and (b) DTG curves of LDH, APP, and compound; Fig. S4: the particle size of Mg–Al-LDH; Fig. S5: XRD patterns of pure EVA and pure APP; Table S1: variance report of tensile test results. See DOI: https://doi.org/10.1039/d6ra00909c.

Acknowledgements

This research was funded by the National Natural Science Foundation of China (Grant No. 92162214) and Science and Technology of Program Qinghai (2023-ZJ-752), Anhui University (Startup Fund-China S020318008/001, Startup Fund-China S020318008/021).

References

1 N. S. Allen, M. Edge, M. Rodriguez, *et al.*, Aspects of the thermal oxidation of ethylene-vinyl acetate copolymer, *Polym. Degrad. Stab.*, 2000, **68**(3), 363–371.
2 M. Fu and B. Qu, Synergistic flame retardant mechanism of fumed silica in ethylene-vinyl acetate/magnesium hydroxide blends, *Polym. Degrad. Stab.*, 2004, **85**(1), 633–639.
3 M. Maiti, R. V. Jasra, S. K. Kusum, *et al.*, Microcellular foam from ethylene vinyl acetate/polybutadiene rubber (EVA/BR) based thermoplastic elastomers for footwear applications, *Ind. Eng. Chem. Res.*, 2012, **51**(32), 10607–10612.
4 A. L. D. Róz, A. M. Ferreira, F. M. Yamaji, *et al.*, Compatible blends of thermoplastic starch and hydrolyzed ethylene-vinyl acetate copolymers, *Carbohydr. Polym.*, 2012, **90**(1), 34–40.
5 Z. Tiefeng, W. Chunfeng, W. Yongliang, Q. Lijun and H. Zhidong, Enhanced Flame Retardancy in Ethylene–Vinyl Acetate Copolymer/Magnesium Hydroxide/Polycarbosilane Blends, *Polymers*, 2021, **14**(1), 36, DOI: 10.3390/POLYM14010036.
6 G. Xiping, Z. Pan, Y. Dahu, L. Chang, Y. Ruiheng and S. Qi, Regulating the Localization of Intumescent Flame Retardant for Improving the Flame Retardancy of Ethylene-vinyl Acetate Copolymer Using Polyamide 6 as a Charring Agent, *J. Wuhan Univ. Technol., Mater. Sci. Ed.*, 2023, **38**(3), 701–711, DOI: 10.1007/S11595-023-2749-6.
7 J. W. Jiang, R. F. Guo, H. F. Shen and S. Y. Ran, Phosphine oxide for reducing flammability of ethylene-vinyl-acetate copolymer, *E-Polymers*, 2021, **21**(1), 299–308, DOI: 10.1515/epoly-2021-0027.
8 H. Jose, Y. GuangZhong, Y. Xiaoli, Z. Xiaodong, P. S. Gonzalez, A. Xiang and W. DeYi, Synergistic Effect of Cerium Oxide for Improving the Fire-Retardant, Mechanical and Ultraviolet-Blocking Properties of EVA/Magnesium Hydroxide Composites, *Materials*, 2022, **15**(17), 5867, DOI: 10.3390/MA15175867.

9 Y. Liang, J. Xu, N. Ahmed, J. Shi, M. Wen and N. Yan, Construction of biomass-based flame-retardant, antimicrobial and hydrophobic wood coatings with POSS organic-inorganic nanoparticles, *Eur. Polym. J.*, 2024, **219**, 113370, DOI: 10.1016/j.eurpolymj.2024.113370.
10 C. Cheng, Z. Zhu, M. Wang, H. Sun, J. Li, R. Jiao and A. Li, Enhanced flame retardancy and thermal insulation of epoxy resins composites incorporated with ammonium polyphosphate and ionic liquids loaded CuO-ZnO hollow spheres, *Colloids Surf., A*, 2024, **703**, 135388, DOI: 10.1016/j.colsurfa.2024.135388.
11 C. Baoyu, C. Jiehu, L. Chang, F. Jiamin, W. Shuxia, D. Xiuhong and L. Zhen, Synthesis of MgAl-LDH from three alkali sources for boosting flame retardancy of EP with APP, *Constr. Build. Mater.*, 2024, **447**, 137997, DOI: 10.1016/j.conbuildmat.2024.137997.
12 Q. Chen, S. Xu, R. Li, B. Sun, H. Fang and Q. Zhang, Synthesis of highly dispersed magnesium hydroxide and its application in flame-retardant EVA composites, *RSC Adv.*, 2025, **15**(16), 12854–12865, DOI: 10.1039/d5ra01067e.
13 Y. Liu, B. Li, M. Xu and L. Wang, Highly Efficient Composite Flame Retardants for Improving the Flame Retardancy, Thermal Stability, Smoke Suppression, and Mechanical Properties of EVA, *Materials*, 2020, **13**(5), 1251, DOI: 10.3390/ma13051251.
14 L. H. Ai, S. S. Chen, J. M. Zeng, L. Yang and P. Liu, Synergistic Flame Retardant Effect of an Intumescent Flame Retardant Containing Boron and Magnesium Hydroxide, *ACS Omega*, 2019, **4**(2), 3314–3321, DOI: 10.1021/acsomega.8b03333.
15 C. Ma, B. Yu, N. N. Hong, Y. Pan, W. Z. Hu and Y. Hu, Facile Synthesis of a Highly Efficient, Halogen-Free, and Intumescent Flame Retardant for Epoxy Resins: Thermal Properties, Combustion Behaviors, and Flame-Retardant Mechanisms, *Ind. Eng. Chem. Res.*, 2016, **55**(41), 10868–10879, DOI: 10.1021/acs.iecr.6b01899.
16 L. H. Ai, L. Yang, J. F. Hu, S. S. Chen, J. M. Zeng and P. Liu, Synergistic Flame Retardant Effect of Organic Phosphorus-Nitrogen and Inorganic Boron Flame Retardant on Polyethylene, *Polym. Eng. Sci.*, 2020, **60**(2), 414–422, DOI: 10.1002/pen.25296.
17 L. Jin, Q.-J. Huang, H.-Y. Zeng, J.-Z. Du and S. Xu, Organic modification of Mo-decorated MgAl layered double hydroxide for polymer flame retardancy, *Composites, Part A*, 2020, **129**, 105717, DOI: 10.1016/j.compositesa.2019.105717.
18 L. Jin, H.-Y. Zeng, J.-Z. Du and S. Xu, Intercalation of organic and inorganic anions into layered double hydroxides for polymer flame retardancy, *Appl. Clay Sci.*, 2020, **187**(C), 105481, DOI: 10.1016/j.clay.2020.105481.
19 Z. Tiefeng, W. Chunfeng, W. Yue, W. Yongliang and H. Zhidong, Effects of Modified Layered Double Hydroxides on the Thermal Degradation and Combustion Behaviors of Intumescent Flame Retardant Polyethylene Nanocomposites, *Polymers*, 2022, **14**(8), 1616, DOI: 10.3390/POLYM14081616.
20 T. Kuila, H. Acharya, S. K. Srivastava, *et al.*, Synthesis and characterization of ethylene vinyl acetate/Mg–Al layered double hydroxide nanocomposites, *J. Appl. Polym. Sci.*, 2007, **104**(3), 1845–1851.
21 J. Du, L. Jin, H. Zeng, *et al.*, Facile preparation of an efficient flame retardant and its application in ethylene vinyl acetate, *Appl. Clay Sci.*, 2019, **168**, 96–105.
22 L. Yuan, G. Yanshan, Z. Zhang and W. Qiang, Preparation of ammonium polyphosphate and dye co-intercalated LDH/polypropylene composites with enhanced flame retardant and UV resistance properties, *Chemosphere*, 2021, **277**, 130370, DOI: 10.1016/J.CHEMOSPHERE.2021.130370.
23 Y. Feng, H. Wang, B. Zhang, *et al.*, Effect of different surface modifiers on the flame retardancy of ethylene-vinyl acetate copolymer/polyethylene/magnesium hydroxide composite systems, *J. Appl. Polym. Sci.*, 2024, **141**(41), e56061.
24 M. Lingyu, L. Xiangrui, L. Mingli, L. Chunfeng, M. Lipeng and H. Sen, Modified Ammonium Polyphosphate and Its Application in Polypropylene Resins, *Coatings*, 2022, **12**(11), 1738, DOI: 10.3390/COATINGS12111738.
25 Y. Chen, S. Yi, X. Zhang, D. Shi, C. Liu, P. Rao and C. Huang, Study on flame retardancy of EPDM reinforced by ammonium polyphosphate, *RSC Adv.*, 2024, **14**(13), 8684–8694, DOI: 10.1039/D4RA00733F.
26 W. Zhiwen, J. Yan, Y. Xiaomei, Z. Junhuan, F. Wanlu, W. Na and W. DeYi, Surface Modification of Ammonium Polyphosphate for Enhancing Flame-Retardant Properties of Thermoplastic Polyurethane, *Materials*, 2022, **15**(6), 1990, DOI: 10.3390/MA15061990.
27 J. Zhanyou, M. Jianzhong, W. Huidi, F. Guiqiang, C. Mengyuan, L. Zengbo, W. Ce, Z. Guohong and S. Liang, The effect of MgAl-LDH/APP distribution control in the closed-cell structure of SBR/EVA foam on flame retardance and mechanical properties, *Polym. Degrad. Stab.*, 2023, **212**, DOI: 10.1016/J.POLYMDEGRADSTAB.2023.110354.
28 Z. Wang, B. Zhang and P. Jiang, Flammability and mechanical properties of EVA composites containing ammonium polyphosphate microcapsules, *Adv. Mater. Res.*, 2012, **1669**(466–467), 267–271.
29 A. A. G. Sowndarya, M. Sujata and R. Prasanna, Phosphate intercalated Mg/Al layered double hydroxide nanosheets as a novel flame retardant for leather: Synthesis, characterization, and application studies, *Appl. Clay Sci.*, 2022, **230**, DOI: 10.1016/J.CLAY.2022.106714.
30 S. Xu, M. Zhang, S. Y. Li, H. Y. Zeng, J. Z. Du, C. R. Chen, K. Wu, X. Y. Tian and Y. Pan, The effect of ammonium polyphosphate on the mechanism of phosphorous-containing hydrotalcite synergism of flame retardation of polypropylene, *Appl. Clay Sci.*, 2020, **185**, 105348, DOI: 10.1016/j.clay.2019.105348.
31 L. Wang, M. Xu, B. Shi, B. Li and S. Invernizzi, Flame Retardance and Smoke Suppression of CFA/APP/LDHs/EVA Composite, *Appl. Sci.*, 2016, **6**(9), DOI: 10.3390/app6090255.
32 Z. Zhenya, Y. Mingcheng, C. Kunpeng, C. Yang, L. Shubo, L. Wentao and L. Jilin, Effect of the Flame Retardants and Glass Fiber on the Polyamide 66/Polyphenylene Oxide Composites, *Materials*, 2022, **15**(3), 813, DOI: 10.3390/MA15030813.

33 H. Ning, Z. Ma, Z. Zhang, D. Zhang and Y. Wang, Core–shell expandable graphite @ layered double hydroxide as a flame retardant for polyvinyl alcohol, *J. Therm. Anal. Calorim.*, 2021, **147**(11), 1–10, DOI: 10.1007/S10973-021-10843-X.

34 Z. Liangliang, N. Kangren, W. Haotian, W. Jiamin, L. Meihong, L. Yafang and Y. Li, Char formation and smoke suppression mechanism of montmorillonite modified by ammonium polyphosphate/silane towards fire safety enhancement for wood composites, *Wood Sci. Technol.*, 2024, **58**(2), 811–827, DOI: 10.1007/S00226-024-01546-1.

35 J.-Z. Du, L. Jin, H.-Y. Zeng, B. Feng, S. Xu, E.-G. Zhou, X.-K. Shi, L. Liu and X. Hu, Facile preparation of an efficient flame retardant and its application in ethylene vinyl acetate, *Appl. Clay Sci.*, 2019, **168**, 96–105, DOI: 10.1016/j.clay.2018.11.004.

36 Z. Shaojie, Q Yi, C. Xilei and L. Long, In situ synthesis of layered double hydroxides-silicon dioxide hybrids and its flame retardancy in EVA composites, *J. Therm. Anal. Calorim.*, 2018, **134**(2), 1071–1082, DOI: 10.1007/s10973-018-7331-7.

37 W. Yuguang, L. Guodong, Z. Liqing, S. Jingquan and Z. Jinlong, Influence of ammonium polyphosphate on flame-retardant behavior and smoke suppression property of EVA/magnesium hydroxide composites, *Ferroelectrics*, 2018, **523**(1), 1–13, DOI: 10.1080/00150193.2018.1391528.

38 C. Baoyu, C. Jiehu, L. Chang, F. Jiamin, W. Shuxia, D. Xiuhong and L. Zhen, Synthesis of MgAl-LDH from three alkali sources for boosting flame retardancy of EP with APP, *Constr. Build. Mater.*, 2024, **447**, 137997, DOI: 10.1016/J.CONBUILDMAT.2024.137997.

39 L. Shaoquan, Z. Xiaodong, L. Long, Q. Yi, G. Qingjie and M. Jingjing, Synthesis of LDHs Based on Fly-Ash and Its Influence on the Flame Retardant Properties of EVA/LDHs Composites, *Polymers*, 2022, **14**(13), 2549, DOI: 10.3390/POLYM14132549.

40 D. N. JitaoJi, Z. Y. YanqinShi, S. Z. MengMa and A. XuWang, simple method for preparing flame retardancy EVA/POE-g-MAH composites with high tensile strength by modified magnesium hydroxide and aluminum hydroxide, *J. Appl. Polym. Sci.*, 2024, **141**(24), DOI: 10.1002/APP.55505.

41 X. Dong, X. Yang, S. Wang, K. Wang, Y. Zhang, J. Liu and H. Chang, Concurrently improving fire safety and processability of ethylene vinyl acetate copolymer by expandable graphite and polyphosphoric acid, *Polym. Compos.*, 2023, **44**(10), 7017–7029, DOI: 10.1002/PC.27615.

42 S. Xu, M. Zhang, S.-Y. Li, H.-Y. Zeng, J.-Z. Du, C.-R. Chen and Y. Pan, The effect of ammonium polyphosphate on the mechanism of phosphorous-containing hydrotalcite synergism of flame retardation of polypropylene, *Appl. Clay Sci.*, 2019, **185**, 105348, DOI: 10.1016/j.clay.2019.105348.

43 L. Zeng, L. Yang, L. Ai, Z. Ye and P. Liu, Synergistic Flame Retardant Effect of Ammonium Polyphosphate and Aluminum Hydroxide on Polyurethane, *J. Wuhan Univ. Technol., Mater. Sci. Ed.*, 2022, **37**(3), 533–539, DOI: 10.1007/s11595-022-2562-7.

44 F. Laoutid, L. Bonnaud, M. Alexandre, J. M. Lopez-Cuesta and P. Dubois, New prospects in flame retardant polymer materials: From fundamentals to nanocomposites, *Mater. Sci. Eng., R*, 2009, **63**(3), 100–125, DOI: 10.1016/j.mser.2008.09.002.

45 T. Zhang, C. Wang, Y. Wang, Y. Wang and Z. Han, Effects of Modified Layered Double Hydroxides on the Thermal Degradation and Combustion Behaviors of Intumescent Flame Retardant Polyethylene Nanocomposites, *Polymers*, 2022, **14**(8), 1616, DOI: 10.3390/polym14081616.